Separation and Purification Technology 210 (2019) 698–709

Contents lists available at ScienceDirect

Separation and Purification Technology

journal homepage: www.elsevier.com/locate/seppur

Fast decolourization of Indigo Carmine and Crystal Violet in aqueous environments through micellar catalysis

Adina Răducan[a], Mihaela Puiu[a,*], Petruţa Oancea[a], Claudiu Colbea[a], Andrei Velea[a], Bogdan Dinu[a], Ana Maria Mihăilescu[a], Toma Galaon[b]

[a] Department of Physical Chemistry, University of Bucharest, 4-12 Elisabeta Blvd., 030018 Bucharest, Romania
[b] National Research and Development Institute for Industrial Ecology – INCD-Ecoind, 71-73 Drumul Podu Dambovitei, Bucharest, Romania

ARTICLE INFO

Keywords:
Surfactant
Micelle
Indigo carmine
Crystal violet
Bicarbonate-activated peroxide
Oxidation

ABSTRACT

Herein we report the modulating effect of sodium dodecyl sulphate (SDS), hexadecyl-pyridinium chloride (HDPC) and octylphenol ethoxylate (Triton X100) on the degradation of indigo carmine (IC) and crystal violet (CV) in bicarbonate-activated peroxide (BAP) system. Upon the addition of surfactant/BAP "surfoxidant", the decolourization degrees of both dyes were above 60% after 5 min, and the total organic carbon removal after 15 min varied within 44–50%. While SDS has shown rather an inhibitory effect during the oxidation of CV, HDPC and Triton promoted the oxidation of both CV and IC, particularly HDPC when a 10-fold increase of the decolourization rate was obtained. This behaviour suggests the formation of active entities –kinetic micelles- acting as nano-reactors by "enclosing" reactants in small-sized aggregates with volumes ranging from 30 to 720 nm^3.

1. Introduction

Synthetic and natural dyes used at industrial scale, though they display significant structural diversity, can be divided in several main classes: azo, indigoid, anthraquinone, sulphur, triphenylmethyl (trityl) and phthalocyanine [1]. Most of them are highly toxic and resistant to microbial attack and present high stability to light, heating, and oxidation [2]. The current technologies for colour removal include adsorption on inorganic/organic matrices, photocatalysis, oxidation [3] and enzymatic decomposition [4]. The advanced oxidation/reduction processes (AO/RPs), which primarily involve the formation of hydroxyl radical ˙OH, as the oxidizing species and hydrated electron/ hydrogen atom as the reducing species, may yield complete mineralization of oxidation-recalcitrant xenobiotics and pharmaceutics at ambient temperature [5–7]. ˙OH·is the second highest powerful oxidant after fluorine, attacking most of the organic molecules at near diffusion-limited rates [8], but is not particularly selective. Most AO/RPs rely on generation of ˙OH from hydrogen peroxide through electron transfer to iron ions, which act as homogenous catalysts [2]. A major issue of AO/RPs is the presence of the bicarbonate anion (HCO_3^-) in surface and wastewater; bicarbonate scavenges ˙OH yielding another ROS, less reactive than OH, the carbonate radical $^{\cdot}CO_3^-$ [9]. The pre-treatment procedures for bicarbonate removal are costly and technically demanding. On the other hand, the generation of multiple ROS through the reaction of HCO_3^- and H_2O_2 in ambient conditions may be a convenient method to overcome AOP limitations in destructing oxidation-resistant pollutants in aqueous environment (Eqs. (1)–(9)) [10].

$$H_2O_2 + HCO_3^- \rightleftarrows HCO_4^- + H_2O \quad (1)$$

$$HCO_4^- \rightarrow \cdot CO_3^- + \cdot OH \quad (2)$$

$$HCO_3^- + \cdot OH \rightarrow \cdot CO_3^- + H_2O \quad (3)$$

$$\cdot CO_3^- + H_2O_2 \rightarrow HOO\cdot + HCO_3^- \quad (4)$$

$$HOO\cdot \rightarrow H^+ + O_2^-\cdot \quad (5)$$

$$O_2^-\cdot + HCO_3^- \rightarrow HOO\cdot + CO_3^{2-} \quad (6)$$

$$\cdot OH + H_2O_2 \rightarrow HOO\cdot + H_2O \quad (7)$$

$$CO_3^{2-} + H^+ \rightarrow HCO_3^- \quad (8)$$

$$\cdot OH + \cdot OH \rightarrow H_2O_2 \quad (9)$$

It was found that bicarbonate-activated peroxide system (BAP) is able to efficiently degrade chlorophenols [11], alkenes [12] and arylsulphides [13], relying mostly on the formation of the carbonate radical. $^{\cdot}CO_3^-$ is a strong one-electron oxidant (E^0 = 1.78 V *vs* NHE, pH 7.0, and though less powerful than ˙OH (E^0 = 2.3 V *vs* NHE, pH 7.0),

* Corresponding author.
E-mail address: elenamihaela.puiu@g.unibuc.ro (M. Puiu).

https://doi.org/10.1016/j.seppur.2018.08.052
Received 3 May 2018; Received in revised form 24 July 2018; Accepted 26 August 2018
Available online 27 August 2018
1383-5866/

acts by both electron transfer and hydrogen abstraction to produce free radicals from reducing substrates [14]. However, to ensure steady concentrations of $^{\cdot}CO_3^-$ and other ROS, large amounts of BAP may be required (a molar ratio dye/BAP of $1/10^4$ has been found effective for the removal of several nitrophenolic compounds from aqueous solutions [19]). On the other hand, the BAP system may become efficient for dye degradation, provided that the oxidation rate could be increased in the presence of biodegradable, non-toxic compounds, such as surfactants. Besides dyes, effluents form carpet manufacturing, paint, textile and tannery often contain surfactants [1,15]. Colloidal surfactants are amphiphilic species, able to form small aggregates (micelles) in solutions [16]. These aggregates contain both hydrophobic and hydrophilic regions and may function as nano-reactors by "enclosing" reactants in small volumes ranging from 30 to 720 nm^3, depending of the nature of the surfactant [17,18]. Thus, the reaction rates in micellar environment can differ significantly from those observed in aqueous media, due to solubilization of the reactants, decrease of their effective concentrations, partition of reactants in different 'compartments' within the bulk solution, and changes in the polarity of the different regions of the system [19]. Kinetic laws for reactions occurring in micelles have overall similarities to enzymatic catalysis [16,20]. Micellar kinetic effects are strictly related to the characteristics of the surfactants, their hydrophilic and hydrophobic groups, and to the particular counter-ion [16]. Micellar modulation was often encountered in the degradative processes of synthetic dyes in alkaline media, especially for the triphenylmethyl dyes, malachite green and crystal violet (CV, IUPAC name N-[4-[bis[4-dimethylamino)-phenyl]-methylene]-2,5-cyclohexadien-1-ylidine]-N-methylmethan aminium chloride) [19,21,22], but was less found in the oxidation of indigoid dyes such as indigo carmine (IC, IUPAC name disodium (2E)-3-oxo-2-(3-oxo-5-sulfonato-1,3-dihydro-2H-indol-2-ylidene)-5-indolinesulfonate) [23].

There are no previous papers reporting BAP oxidation of CV or IC, possibly due to the high BAP oxidant/dye molar ratios needed for the BAP system to operate at reasonable oxidation rates. Moreover, BAP oxidation in micellar media was reported only for the oxidation of arylsulphides, with cetyltrimethylammonium bicarbonate as a cationic "surfoxidant" (resulted from the combination of an ionic surfactant with a counter-ion that is itself an oxidant or activates an oxidant from the bulk solution to form an oxidant counter-ion) [13]. In this work we attempted to exploit the possible promoting effects of three biodegradable surfactants: sodium dodecyl sulphate, SDS (anionic), hexadecyl-pyridinium chloride, HDPC (cationic) and octylphenol ethoxylate, Triton X100 (non-ionic) on BAP oxidation of IC and CV. We provided a realistic kinetic model for this type of reaction network, in agreement with the reported micellar catalytic models for composite reactions [22,24].

2. Materials and methods

2.1. Materials

Crystal violet ACS reagent, Indigo carmine of analytical standard grade, sodium bicarbonate (99.5%) sodium dodecyl sulphate (98%), hexadecyl-pyridinium chloride monohydrate (99%) and Triton X100 laboratory grade were purchased from Sigma-Aldrich. Hydrogen peroxide was obtained as a 30% solution from Merck. After dilution with bi-distilled water the concentrations of H_2O_2 solutions were determined spectrophotometrically, using the molar extinction coefficient $\varepsilon_{240\ nm} = 43.6\ M^{-1}\ cm^{-1}$. Stock solutions of 1 mM CV, 1 mM IC, 0.02 M SDS, 20 mM HDPC, 1 mM Triton X100, 1 M H_2O_2 and 0.1 M $NaHCO_3$ were also prepared in bi-distilled water. HPLC grade acetonitrile (ACN) and LC-MS grade formic acid were also acquired from Sigma-Aldrich. Water for chromatography was obtained within the laboratory, by means of a MilliQ instrument. Working standard solutions with a concentration of 20 μg/mL were prepared using water as final diluent from the stock standard solutions by appropriate dilutions. These standard solutions were used to identify the chromatographic peaks of the two dyes using retention time, MS spectra and UV–Vis spectra. All standard solutions and degraded samples were kept protected from light at 4 °C until injection in the LC-MS system.

2.2. Spectrophotometric assays

The ultraviolet–visible (UV–VIS) measurements of CV and IC solutions in the presence of surfactants and during the degradation with the BAP system were performed with a JASCO V-530 spectrophotometer equipped with a Peltier cell for temperature and stirring control.

2.3. Liquid chromatography–mass spectrometry (LC-MS) analysis

Experiments were run using an Agilent 1260 series LC system (Agilent, Waldbronn, Germany) consisting of: binary pump, degasser, thermostated autosampler, thermostated column compartment and diode array detector (DAD) which was coupled with an Agilent 6410B triple-quadrupole mass analyzer with electrospray ionization source (ESI). Data acquisition and analysis were performed using Agilent Mass Hunter software, revision B.07.05. All chromatographic runs were carried out on a Hypersil GOLD (100 × 2.1 mm, 3.0 μm) column from Thermo Scientific. The chromatographic column was thermostated at 35 °C. Isocratic elution was performed with a mobile phase composition of aq. 0.2% formic acid and acetonitrile in the volumetric ratio 60/40. A low mobile phase flow-rate of 0.20 mL/min was chosen to enhance ESI ionization and sensitivity. Chromatograms were recorded for 12 min. Injection volume of 10 μL was used. MS detection of the substrates and their oxidation products was done in full scan mode (MS Scan) in the range 50–400 Da for Crystal Violet and 40–500 Da for Indigo Carmine. Both positive and negative spectra were acquired to observe degradation products for both polarities. ESI ionization source parameters were: drying gas temperature 300 °C, drying gas flow-rate 6.0 L/min, nebulizer pressure 45 psi. Sampling capillary voltage was set to 2500 V for negative mode and 3500 V for positive mode. Skimmer (fragmentor) voltage was set to 90 V and the Cell Accelerator Voltage (Q2) was set to 4 V. UV–VIS detector (DAD) was placed in series before the Triple Quadrupole Mass spectrometer. Detection wavelengths were set at 580, 302, 270 and 240 nm and UV–VIS spectral data was also obtained simultaneously (220–620 nm). Retention time difference of about 0.2 min between UV–VIS and MS chromatograms are due to capillary length between the 2 detectors.

2.4. Degradation experiments

The oxidations were conducted directly in a 3.5 mL spectrophotometer cuvette trough temperature (25 °C) and stirring control. The reaction progress was monitored through the absorbance changes of the dye/surfactant/BAP mixtures at specific wavelengths: 590 nm for CV and 610 nm for IC. The absorbance decrease was used further to estimate the time-evolution of the total conversion. In order to ensure pseudo-first kinetics and to settle the pH at a constant value, in all degradation experiments the concentrations of H_2O_2 and bicarbonate exceeded at least 25-fold the dye concentrations, as it follows:

- the optimized initial concentrations for CV oxidation were $[CV]_0 = 0.4$ mM, $[H_2O_2]_0 = 20$ mM and $[NaHCO_3]_0 = 20$ mM (CV/HCO_3^-/H_2O_2 molar ratio of 1/50/50).
- the optimized initial concentrations for IC oxidation were $[IC]_0 = 0.8$ mM, $[H_2O_2]_0 = 200$ mM and $[NaHCO_3]_0 = 20$ mM (IC/HCO_3^-/H_2O_2 molar ratio of 1/25/250).

The concentration of surfactants were chosen to cover both premicellar and micellar regions, considering the following values for critical micelle concentrations (CMC): $CMC_{(SDS)} = 8.08$ mM [25], $CMC_{(HDPC)} = 0.87$ mM [26] and $CMC_{(Triton\ X100)} = 0.24$ mM [27]. No

pH shifting from the value of 8.5 in the reaction solutions was observed over the reaction time span. LC–MS/UV–VIS analysis was performed first on the bicarbonate solutions of CV and IC, then on the reaction mixtures CV/BAP and IC/BAP after 15 min, when the decolourization degrees exceeded 98%.

2.5. Total organic carbon (TOC) assay

TOC analysis of the dye solutions and of the final oxidation mixtures was performed on an Apollo 900 Combustion TOC Analyzer (Teledyne Tekmar, Mason, Ohio, USA) with a Non-dispersive Infra Red (NDIR) detector for CO_2 (0–20 ppm calibration range). The total combustion of the samples was achieved through the 680 °C combustion catalytic oxidation method. Data processing was performed with the TOC Talk Apollo 9000HS v. 4.2 software. TOC analysis was performed first on the bicarbonate solutions of CV, IC, SDS, HDPC and Triton x 100, then on the reaction mixtures CV/BAP, IC/BAP, SDS/BAP, HDPC/BAP, Triton X100/BAP, CV/SDS/BAP, CV/HDPC/BAP, CV/Triton x 100/BAP, IC/SDS/BAP, IC/HDPC/BAP and IC/Triton x 100/BAP after 15 min, when the decolourization degrees exceeded 98%.

3. Results and discussion

3.1. Separation and identification of BAP oxidation products

LC-MS/UV–VIS analysis of the reaction mixtures after 15 min confirmed the presence of residual organic products from the degradation of both dyes. The results of LC chromatograms, UV–VIS spectra, and LC–ESI mass spectra are summarized in Tables 1 and 2 and in Supplementary Information SI, Figs. SI-1-21.

Supplementary data associated with this article can be found, in the online version, at https://doi.org/10.1016/j.seppur.2018.08.052.

Our results matched well those obtained by Fan an collab [28] during the degradation of CV by Fenton and Fenton-like systems (0.5 mM Fe^{2+}/50 mM H_2O_2 and 1 mM Fe^{3+}/50 mM H_2O_2 for 0.15 mM CV, at pH 3). We have noticed that BAP oxidation of CV follows a similar reaction pattern, through the *N*-de-methylation of CV (see Scheme 1).

4-(*N*,*N*-dimethylamino)phenol was not found in the reaction mixture through LC-MS analysis, possibly due to its complete mineralization, as it was reported for the BAP oxidation of aminophenols [10].

On the other hand, the degradation products of BAP oxidation of IC were similar to those obtained during the photocatalytic degradation of IC by composites containing nanometric SnO_2 supported on Al_2O_3 [29] and during the chemical degradation of IC with MnO_2/ natural Fique fiber bionanocomposite [30]. Their proposed reaction pathway indicated the formation of product ions from the release of small molecules as CO, CO_2, and H_2O (see Scheme 2).

The proposed degradation scheme involved the formation of isatin-5-sulfonic acid via 2-hydroxy-2′ hydroperoxy-Indigo-5,5′-disulfonic acid [31]; even if isatin-5-sulfonic acid was not identified in the final reaction mixture; it appears that the cleavage of the di-oxo-indoline ring ultimately yielded 4-aminohydroxybenzenesulfonic acid. The electron withdrawing effect of the C-1 sulfonic group tends to stabilize the aromatic ring and to block the formation of *o*-quinone imine (C-3 and C-4), a key component observed in the BAP degradation of 2-aminophenol and 2-amino-4nitrophenol [10].

3.2. Spectral changes through the interaction of CV and IC dyes with surfactants in pre- and micellar conditions

After investigating the UV–VIS spectra of both CV and IC, sharp and well-defined absorption peaks at $\lambda = 590$ nm for CV and for IC at $\lambda = 610$ nm were observed; they were used further to build the calibration lines, providing the extinction coefficients $\varepsilon_{CV} = (182095 \pm 37)\ M^{-1}\,cm^{-1}$ and $\varepsilon_{IC} = (1296.4 \pm 6.8)\ M^{-1}\,cm^{-1}$. Even if the maximum absorbance wavelength for the aqueous solution of CV was at 590 nm, a shoulder peak was also observed; this fact is in agreement with previous studies assigning this spectral pattern to the presence of two isomers in equilibrium, one with a propeller structure (D3 symmetry) for the ground state, and the other one with a pyramidal structure (C3 symmetry), in which three bonds of the central atom are bent [32]. The recorded spectra of CV in the presence of surfactants are summarized in Figs. SI 21-A-C. The spectral changes following the addition of the surfactant to an aqueous solution of triphenylmethyl dye depend on the concentrations of both dye and surfactant and on the nature of the surfactant [33].

The addition of SDS at concentrations below CMC induced significant variations in the absorption spectrum of CV; thus, the peak shoulder observed at $\lambda = 532$ nm increases simultaneously with the reduction of the main peak at $\lambda = 590$ nm (Fig. 1-A).

The increase of SDS concentration up and above CMC, restored the initial shape of the CV spectrum. These observations are consistent with other studies, reporting the appearance of new absorption bands of CV in the premicellar region (where SDS exists as monomer) due to the formation of ion-pair complexes CV-SDS [34,35]. Above CMC, the complex between CV and SDS became unstable, probably due to aggregation of surfactants; moreover, van der Waals interaction between the micelles and the organic moiety of dye could also change the chromophore microenvironment [36,37]. The addition of HDPC did not modify the form of CV spectra (Fig. SI 21-B), and the absorbance values at $\lambda = 590$ nm displayed a minimum around cmc of HDPC (Fig. 1-B), suggesting that CV was inserted in the micellar core [37]. The addition of Triton X100 caused an increase of absorbance at $\lambda = 590$ nm (Fig. SI 21-C and Fig. 1 –C); this increase may be assigned to the interactions between the dye and the non-ionic micelles, with the non-polar region of the dye being localized in the hydrophobic core of the micelle [38].

In the case of IC, the maximum absorbance wavelength for aqueous solution was observed at $\lambda = 610$ nm (Fig. 2 A-C). The recorded spectra of IC in the presence of surfactants are presented in Fig. SI 22-A-C. The addition of HDPC caused the appearance of a new absorption band located at lower wavelength ($\lambda = 560$ nm) (Fig. SI 22-B).

IC in solution is in anionic form; therefore, IC may react with the cationic surfactant. The new band observed at high HDPC

Table 1
Molecular masses and characteristic *m/z* ions of the degradation products of CV/BAP system observed with positive MS polarity.

Compound	Characteristic MS line (*m/z*)	Fragment molecular mass (Da)	λ_{max} (nm)
Crystal violet *N*, *N*, *N′*, *N′*, *N″*, *N″*-hexamethylpararosaniline	372.3 (not found)	371.3 (not found)	588.2 (not found)
4-(*N*,*N*-dimethylamino)-4′-(*N′* ,*N′*-dimethylamino)benzophenone	269.3	268.3	376.4
4-(*N*,*N*-dimethylamino)-4′-(*N′*-methylamino)benzophenone	255.2	254.2	366.6
4-(*N*-methylamino)-4′-(*N′*-methylamino)benzophenone and d 4-(*N*,*N*-dimethylamino)-4′-aminobenzophenone	241.2	240.2	364.4 and 358.8
4-(*N*-methylamino)-4′-aminobenzophenone	227.0	226.0	357.3
4-(*N*,*N*-dimethylamino)phenol	138.2	137.2	309.7

Table 2
Molecular masses, characteristic *m/z* ions and maximum absorbance wavelength of the degradation products of IC/BAP system observed with negative MS polarity.

Compound	Characteristic MS line (*m/z*)	Fragment molecular mass (Da)	λ_{max} (nm)
Indigo Carmine	421 (single charged molecular ion)	422 (sulfonic acid)	609.5 (not found)
Indigo-5,5′-disulfonic acid (disodium salt)	210 (double charged molecular ion)	466 (disodium salt)	
	not found	not found	
Isatin-5-sulfonic acid	226 (not found)	227	260 and 302
(2-amino-5-sulfophenyl) -oxo-ethanoic acid	244	245	260 and 302
2-hydroxy-2′ hydroperoxy-Indigo-5,5′-disulfonic acid (disodium salt)	235.1 (double charged molecular ion)	518.2 (disodium salt)	257 and 302
Product obtained through CO elimination from Isatin-5-sulfonic acid (2-amino-5-sulfobenzoic acid)	216.1	217.1	257 and 302
Product obtained through CO elimination from 216 fragment (possibly 4-amino-3-hydroxybenzenesulfonic acid	188	189	230

concentration could be attributed to the formation of IC-HDPC complex, this effect being reported also for other cationic surfactants [39]. The addition of Triton X100 and SDS had no effect on the absorption spectra, indicating that there were no strong interactions between IC and the surfactant. The electrostatic repulsions between the same charged dye and the SDS particles are stronger than the other interactions, so no stable complex could be stabilized in solution. The addition of Triton X100 caused a slight decrease of the absorption peak due to the formation of dye-surfactant complex and to the incorporation of IC deep into the core of micelles [15].

3.3. Catalytic action of surfactants on BAP/CV and BAP/IC systems

Oxidations of crystal violet and indigo carmine were followed by monitoring the loss of dye absorbance at $\lambda = 590$ nm for CV and $\lambda = 610$ nm for IC in the presence of excess hydrogen peroxide and sodium bicarbonate. We defined the decolourization (conversion) degree as:

$$\frac{A_0 - A}{A_0} \times 100 \quad (10)$$

where A_0 is the value of the absorption peak at specific wavelength for each dye in BAP solution at the beginning of the experiment, and A is the actual peak value. As shown in Figs. 1 and 2, the dye absorption peaks at specific wavelength are strongly dependent on surfactant concentration. For example, when the surfactant is at CMC, the dye is extracted into the micelles, causing a change in the absorbance of dye. Therefore, to accurately calculate the conversion degree in the presence of surfactants, the initial value A_0 was recorded separately replacing H_2O_2 from BAP with H_2O. Thus, the dye/bicarbonate optimized ratio was maintained and the decolourization of dye was prevented.

While both dyes interact with surfactants *via* monomer dye-surfactant complex and/or micellar complex, the addition of surfactant would modify the BAP –oxidation rate of CV and IC. Reaction rates are usually affected in the presence of surfactants, even in pre-micellar region, suggesting that reactants may interact with small sub-micellar aggregates of the surfactant (dimers, trimers, tetramers, etc.), forming active entities (kinetic micelles) [40,41]. First, we investigated the effect of dye, H_2O_2 and bicarbonate concentrations on the decolourization rate (data not shown) in order to estimate the empirical partial reaction orders with respect to each reactant and to provide the dye/BAP molar ratios corresponding to the highest decolourization degree. The rate equations obtained in initial conditions were not factorizable, indicating complex kinetics, due to the intricate chemistry of the BAP system. Therefore, we focused our work on settling the dye/H_2O_2/bicarbonate molar ratio providing the highest decolourization rate. Under the optimized dye/BAP molar ratios, the decolourization process went relatively fast in aqueous solution, while in the presence of surfactants the kinetic behaviour followed different patterns, depending on the nature of the surfactants, the pre-micellar and micellar concentrations (Figs. 3 and 4). The oxidation by H_2O_2 in the absence of bicarbonate was negligible since the dye decolourization was below 5% at the end of each experiment.

High decolourization degrees (90–98%) were obtained after 400–900 s for both dyes. In the case of CV, it appears that the increase of SDS concentration caused a significant decrease of conversion (Fig. 3-A), especially above CMC, suggesting that incorporation of CV into micelles may prevent the access of the generated ROS to the CV substrate. This fact may be assigned to the repulsive interaction among the negatively charged species ($^{\cdot}CO_3^{-}$ and $O_2^{-\cdot}$) and negatively charged SDS. CV is positively charged under experimental conditions and forms ion pairs with SDS. On the other hand, the positively charged HDPC facilitates the access of the negatively charged ROS to CV and this may explain the increase of the decolourization degree, around and above CMC (Fig. 3-B). The non-ionic surfactant Triton X100 displayed a similar behaviour in the absence of electrostatic repulsions for ROS; the high conversions obtained around and above CMC suggested that incorporation of CV into a micellar “compartment” may increase the number of collisions among CV molecules and ROS (the micellar cage effect) [42] and allows the access of negatively charged radicals to the positively charged dye (Fig. 3–C).

Indigo carmine is negatively charged in the experimental environment. The interaction with SDS seems to increase the BAP oxidation rate, especially in the micellar region. Unlike CV, which undergoes electrostatic attraction to SDS, IC doesn’t form ion pairs with SDS and this may be one reason for the higher conversions obtained above CMC, compared to the pre-micellar and aqueous conditions (Fig. 4-A and B). On the other hand, Triton X100 may not prevent charged radicals to reach the anionic dye, but repulsive electrostatic interactions between negatively charged radicals and negatively charged IC may account the moderate increase of conversion in the presence of Triton X100 compared to the “jump” of conversion in the presence of HDPC (Fig. 4-B and C).

3.4. Testing the pseudo-phase model on BAP/CV and BAP/IC systems

One of the most used model for reaction in micellar and pre-micellar media is the pseudo-phase model [24]. According to this model, the distribution of surfactant between different states of aggregation is controlled by a series of cooperative dynamic association-dissociation equilibriums, which can be considered as global steps for the formation of micelles. The reaction occurs both in solution and micelles, according to the following mechanism:

$$nS + D \overset{K_m}{\leftrightarrow} S_nD \quad (11)$$

$$S_nD \overset{k_m[ox]}{\rightarrow} products \quad (12)$$

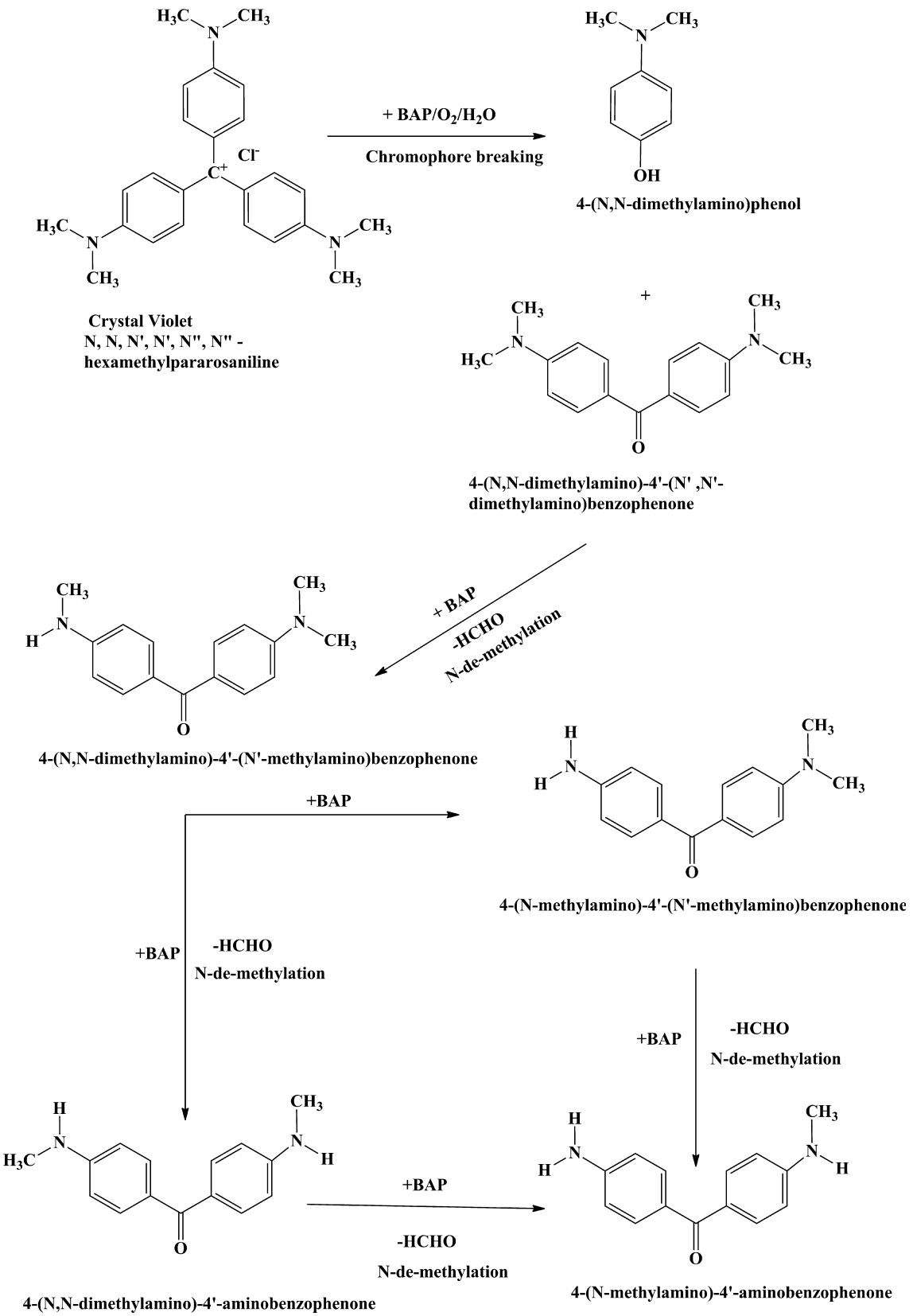

Scheme 1. Proposed degradation pathway of Crystal Violet in bicarbonate activated peroxide system, occurring through cleavage of the chromophoric core and successive N-de-methylation steps.

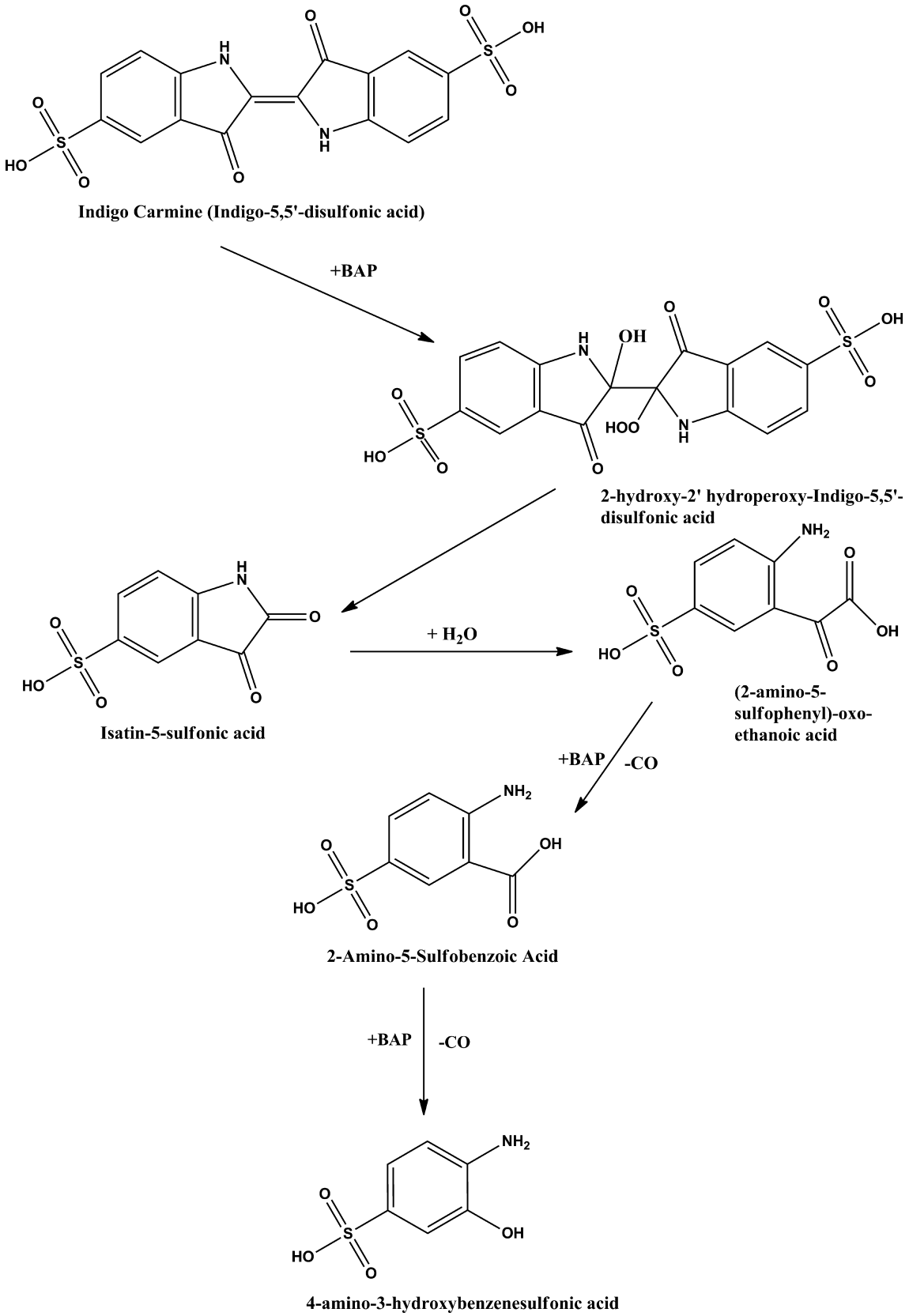

Scheme 2. Proposed degradation pathway of Indigo Carmine in bicarbonate activated peroxide system, through cleavage of the chromophoric core and of the di-oxo-indoline ring.

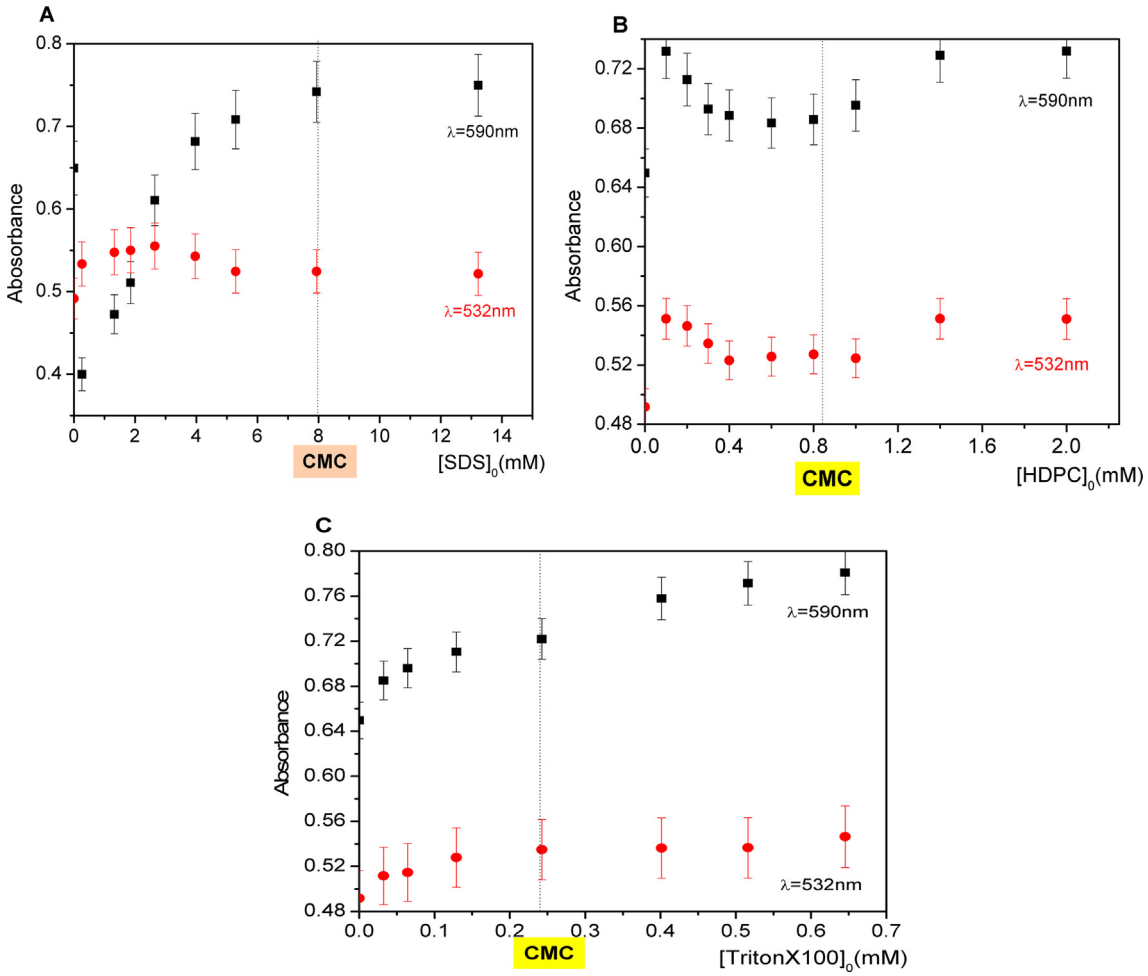

Fig. 1. Influence of surfactant concentration on the VIS absorption peaks of CV below and above CMC: (A) SDS, (B) HDPC and (C) Triton X100. $[CV]_0$ = 0.4 mM, $[NaHCO_3]_0$ = 20 mM.

$$D \xrightarrow{k_{w[ox]}} products \tag{13}$$

where S is the surfactant, D is the dye (CV or IC), n represents the number of surfactant molecules involved in the catalytic act, Km is the dissociation constant of the catalytic micelle SnD, km is the rate constant in micellar phase and kw is the rate constant in aqueous medium.

In these conditions the overall oxidation rate of the dye becomes:

$$-\frac{d[D]}{dt} = r_{w[ox]} + r_{m[ox]} \tag{14}$$

One assumes that due to the large excess of bicarbonate and hydrogen peroxide pseudo-first order kinetics was ensured, providing the rate equation:

$$r_{w[ox]} = k_{w[ox]}[D] \tag{15}$$

For the sequence (11)–(15), the rate equation is derived assuming that step (11) is pre-equilibrated, the micellar complex S_nD is an active intermediate and the concentration of complex S_nD is negligible with respect to the concentration of the unbound surfactant.

$$r_{m[ox]} = k_{m[ox]}[S_nD] = k_{m[ox]}\frac{[S]^n[D]}{K_m} \tag{16}$$

Replacing the rate equations from (15) and (16) to Eq. (14) and taking into account the mass balance equation for S, one obtains:

$$-\frac{d[D]}{dt} = k_{w[ox]}[D] + k_{m[ox]}\frac{[S]_0^n[D]}{K_m} = \left(\frac{k_{m[ox]}[S]_0^n + k_{w[ox]}K_m}{K_m + [S]_0^n}\right)[D] \tag{17}$$

or

$$-\frac{d[D]}{dt} = k_{obs}[D] \tag{18}$$

where $[S]_0$ is the total concentration of surfactant.

According to this model, the oxidation in both aqueous and micellar media follows a pseudo-first order kinetics. For micellar conditions the experimental rate constant k_{obs} has the expression:

$$k_{obs} = k_{w[ox]} + k_{m[ox]}\frac{[S]_0^n}{K_m} \tag{19}$$

This model was applied for other reactions with good results for surfactants concentrations below and above CMC [13,43–45].

The integrated form of Eq. (18) is

$$\frac{[D]}{[D]_0} = e^{-k_{obs}t} \tag{20}$$

or expressed as absorbance ratio

$$\frac{A}{A_0} = e^{-k_{obs}t} \tag{21}$$

The reduced concentration value in Eq. (20) represents the decolourization of dye, and therefore the experimental rate constant k_{obs}, (estimated through non-linear regression) is strictly limited to the decolourization step. We assumed that peroxide, bicarbonate and ROS do not part preferentially into one pseudo-phase [13], due to low polarity of micellar phase [46] and small dimensions of particles. Therefore in was assumed that the pseudo-phase model may reasonably describe the

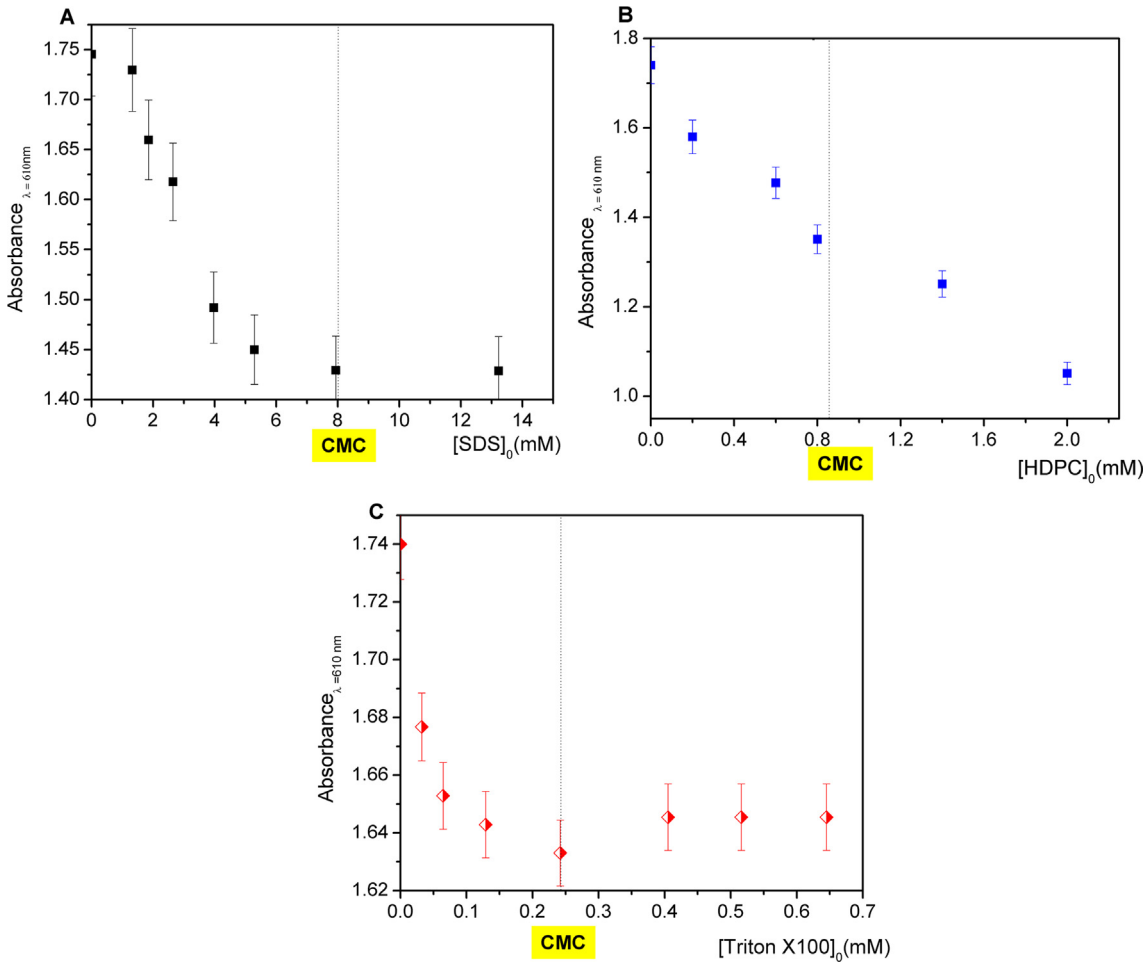

Fig. 2. Influence of surfactant concentration on the VIS absorption peaks of IC below and above CMC: (A) SDS, (B) HDPC and (C) Triton X100. $[IC]_0$ = 0.8 mM, $[NaHCO_3]_0$ = 20 mM.

BAP oxidation of CV and IC in micellar media. According to the pseudo-phase model, and assuming that in aqueous solution, in at least 25-fold excess of BAP, the oxidation of both CV and IC follows a pseudo-first order kinetics, an exponential decay equation would provide the best-fit parameters when fitted on the experimental data absorbance *vs.* time. These assumptions were validated when the non-linear regression analysis of the experimental data provided good correlation parameters (values of the determination coefficient r^2 ranging from 0.9874 to 0.9978 for $\alpha = 0.05$) for the exponential decay equation:

$$\frac{y}{a} = e^{-bx} \tag{22}$$

Thus, the kinetic parameters estimated through non-linear regression analysis were the kinetic constant $k_{w[ox]}$ from the progress curves absorbance *vs.* time obtained in aqueous media, and k_{obs} from the progress curves obtained in the presence of surfactants, according to the pseudo-phase model from Eq. (21) (see the extended kinetic in Figs. SI-23,24 A-C). Comparative plots of k_{obs} obtained in the presence of surfactants at CMC and $k_{w[ox]}$ in aqueous media demonstrate that SDS causes a 10-fold decrease of the CV oxidation rate, while HDPC and Triton X100 ensure around two-fold increase (Fig. 5-A). All three surfactants display a promoting effect on BAP oxidation of IC: 6- fold increased rate for SDS, 9-fold increase for HDPC and 3-fold increase for Triton X100 (Fig. 5-B).

The kinetic parameters of the pseudo-phase models $k_{m[ox]}$, K_m and n were estimated after fitting eq. (15) on the data points k_{obs} *vs.* surfactant concentration (Figs. SI-25-A, B); their values are summarized in Table 3.

The small values of n, indicate the formation of catalytic micelles through specific interactions. The small values of the dissociation constants, K_m, suggested a strong association of dye within the surfactant micelles that may explain the increase of the oxidation rates in micellar environment. The kinetic constants $k_{w[ox]}$ and $k_{m[ox]}$ have the same order of magnitude as in water, aside from the CV-SDS system. Crystal violet was well incorporated into the anionic SDS micelles; the total charge of the micelle was negative, so the approaching of ROS anions could be restrained due to repulsive electrostatic interactions. The other surfactants HDPC and Triton X100 allowed the access of ROS through micelles, therefore increasing the reaction rates. Indigo carmine, as well, was incorporated in cationic HDPC micelles; the total charge of these micelles being positive, the diffusion of ROS through micelles may be favoured, yielding a significant increase of the BAP oxidation rate.

3.5. Quantification of the mineralization level

The analysis of decolourization degrees after 15 min coupled with the LC-MS results demonstrate that BAP system cannot achieve complete mineralization for reasonable dye/BAP molar ratios. The main concern here, as in other similar oxidative water treatments, is the formation of toxic or less biodegradable intermediates/final products. Aromatic compounds with low or moderate toxicity (N-methylated or de-methylated amino-benzophenones, N, N-dimethyl-4-aminophenol) were identified in the final reaction mixture after BAP oxidation of CV (Table 1); similarly, low molecular weight compounds resulting from ring-cleavage and successive elimination of the CO group were obtained

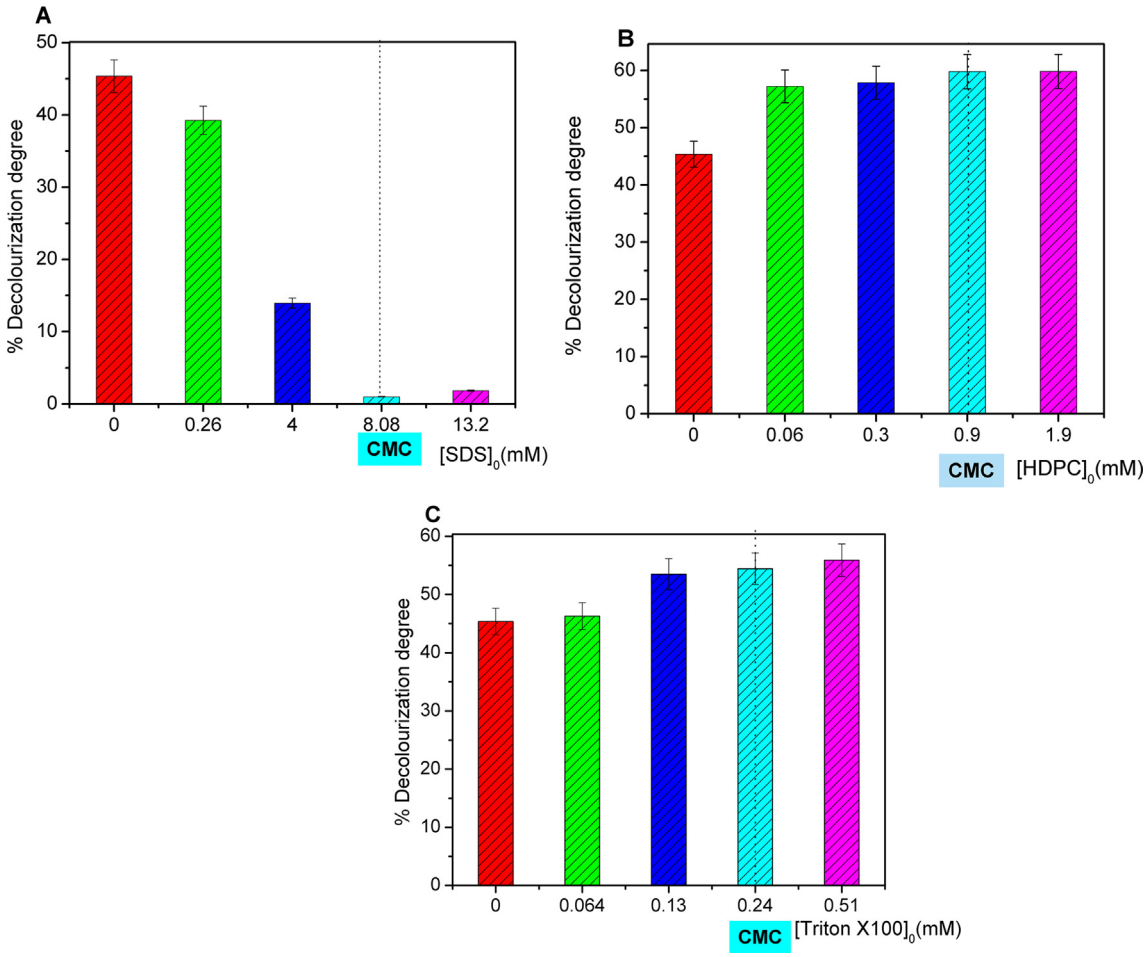

Fig. 3. Variation of CV's decolourization degree after 300 s in the presence of BAP under pre-micellar and micellar conditions: (A) SDS, (B) HDPC and (C) Triton X100. $[CV]_0 = 0.4$ mM, $[NaHCO_3]_0 = 20$ mM, $[H_2O_2]_0 = 20$ mM, T = 25 °C.

during the IC degradation (Table 2). On the other hand, addition of surfactants may "dissipate" the oxidant in "parasitic" oxidative processes involving the surfactants themselves. Therefore, we performed first TOC analysis on CV, IC, SDS, HDPC and Triton X100 in bicarbonate solutions without H_2O_2 (TOC_0) and afterwards on reaction mixtures (with the optimized dye/BAP, surfactant/BAP and dye/surfactant/BAP molar ratios) after 15 min (TOC_∞). The percentage TOC removal was calculated as:

$$\%\ TOC_{removal} = \frac{TOC_0 - TOC_\infty}{TOC_0} \cdot 100 \quad (23)$$

The results (summarized in Table SI-1) suggested that all three surfactants underwent various degrees of mineralization in the presence of BAP: from 17.6% (SDS) to 29.5% (HDPC). TOC removals for both dyes in the absence of surfactants were below 30%. The addition of SDS to CV/BAP mixtures seems to inhibit CV's mineralization (15% TOC removal) which is in agreement with the observed effects of SDS concentration on the overall oxidation rate of CV (Fig. 4-A). On the other hand, HDPC and Triton X 100 increase the mineralization degrees of CV/surfactant mixtures to 44–45%, suggesting that these two surfactants promote not only the cleavage of the chromophoric core of CV (Fig. 4-B and C) but also the mineralization of smaller aminophenolic fragments. In the case of IC, the addition of SDS provided the highest TOC removal (52%), consistent with the promoting effect of SDS on IC decolourization (Fig. 5-A). HDPC seemed efficient for IC's decolourization (Fig. 5-B) but provided similar mineralization degree (around 44%) as Triton X100, even if the former is a weaker promoter of IC's chromophore cleavage (Fig. 5-C). Although moderate mineralization degrees are achieved, it is to be noted that the degradation experiments performed at ambient temperature and at moderate basic pH can be used in a wastewater pre-treatment step, followed by addition of supplementary amounts of hydrogen peroxide in a continuous configuration. Wastewaters from textile plants or tannery already contain various amounts of surfactants that can be used in tandem with the BAP system for dye removal. However, residual SDS and Triton X100 might become sources of secondary pollution, since their TOC removal does not exceed 21%. It was recently reported that several bacterial strains of *Pseudomonas* are able to degrade SDS and Triton X100 [47–49] from soil samples and drainage sediments. For example, *Pseudomonas nitroreducens* is able to degrade and grow with SDS and nitrate or oxygen as electron acceptors [47].

4. Conclusions

The formation of kinetic micelles during the BAP degradation of Crystal Violet and Indigo Carmine in the presence of SDS, HDPC and Triton X100 was confirmed by the matching of the pseudo-phase pattern of micellar catalysis with the obtained kinetic data. The BAP decolourization of Crystal Violet was significantly increased in the micellar environment provided by the cationic HDTC and non-ionic Triton X100 surfactants. The decolourization of Indigo Carmine was accelerated also in the micellar conditions for all three surfactants, but particularly, HDPC cationic micelles displayed the highest promoting activity. Moreover, moderate mineralization degrees of 44–45% were achieved in CV/surfactant mixtures with HDPC and Triton X100, while SDS practically inhibited the BAP oxidation, yielding a TOC removal of

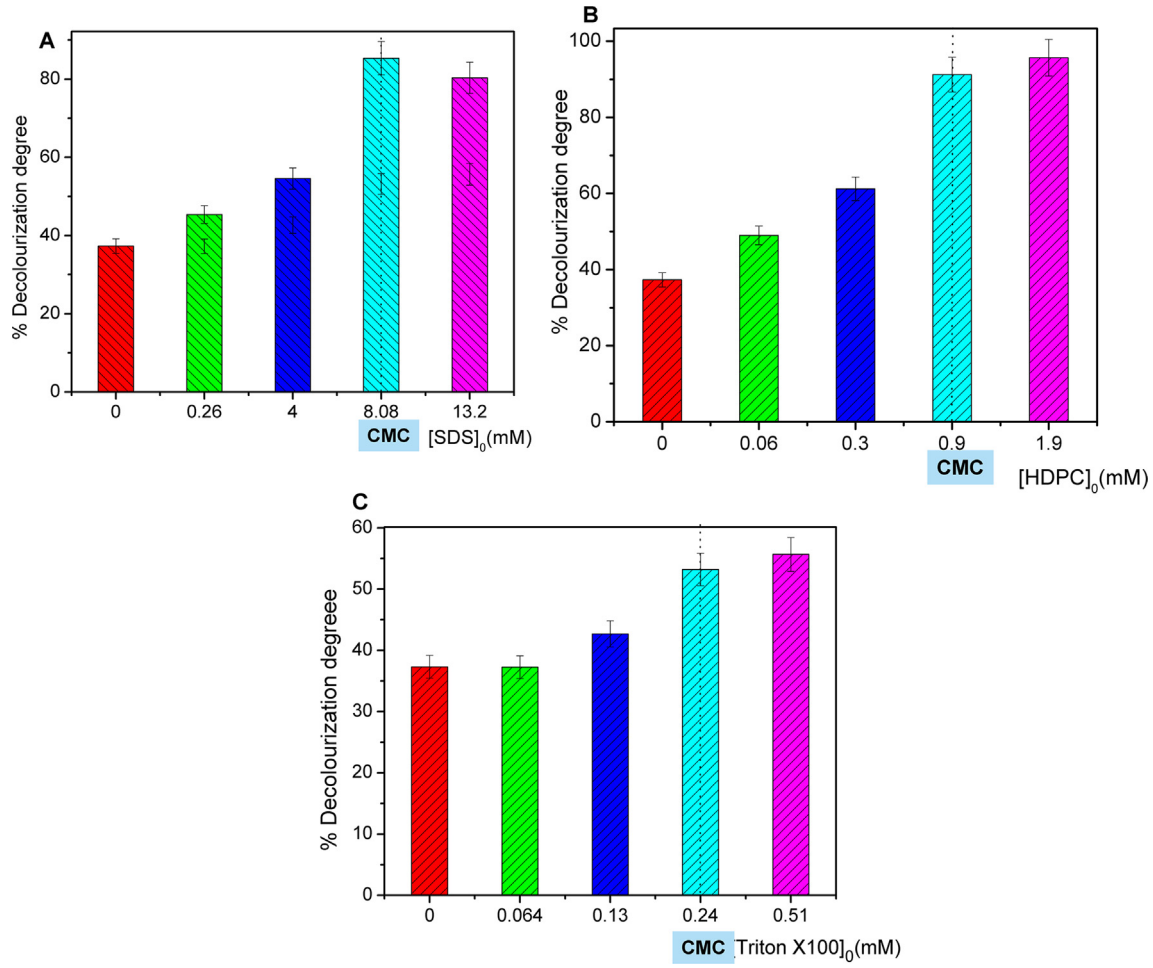

Fig. 4. Variation of IC's decolourization degree after 300 s in the presence of BAP under pre-micellar and micellar conditions (A) SDS, (B) HDPC and (C) Triton X100. $[IC]_0 = 0.8$ mM, $[NaHCO_3]_0 = 20$ mM, $[H_2O_2]_0 = 200$ mM, T = 25 °C.

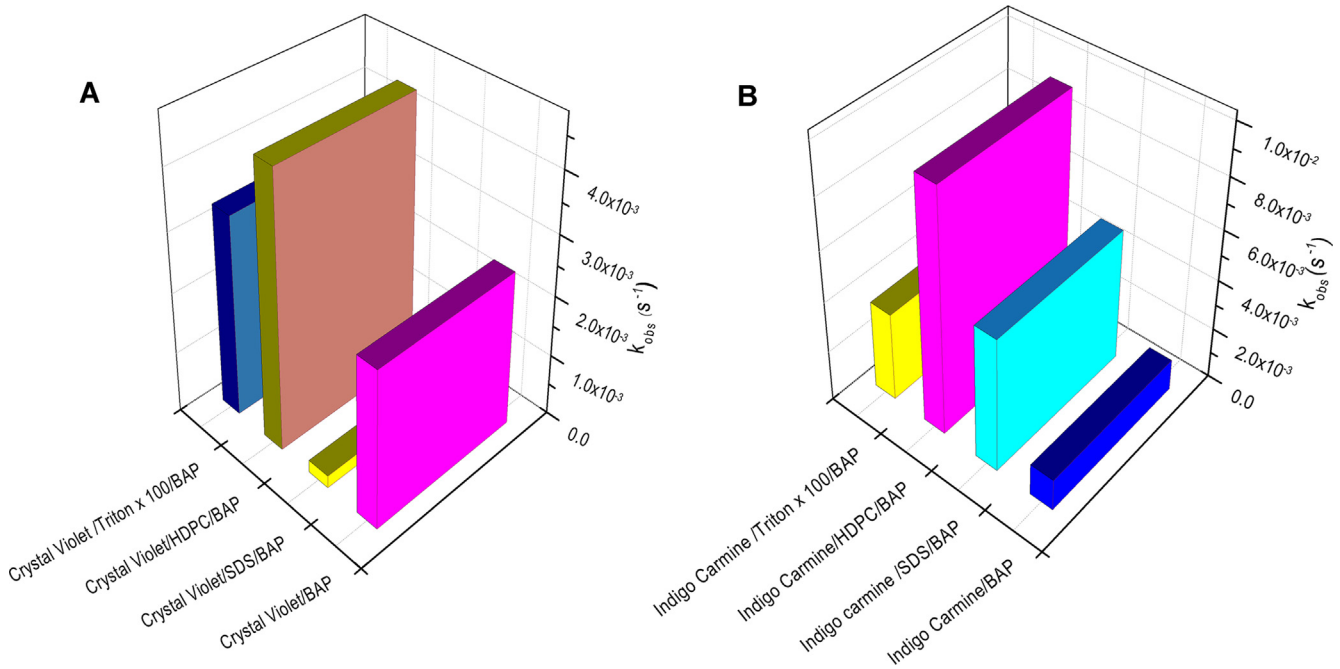

Fig. 5. Catalytic effects of surfactants on BAP oxidation of Crystal Violet (A) and Indigo Carmine (B) expressed as modification of the pseudo-first rate constants in the presence of surfactants in CMC conditions.

Table 3
Estimated kinetic parameters of BAP oxidation of CV and IC in aqueous, pre-micellar and micellar solutions.

Dye	Surfactant	$k_{w[ox]}$ (s^{-1})	$k_{m[ox]}$ (s^{-1})	n	K_m (M)
Crystal Violet	SDS	$(2.55 \pm 0.11)\cdot10^{-3}$	$(3.29 \pm 0.26)\ 10^{-6}$	1.77 ± 0.16	$(2.26 \pm 0.36)\ 10^{-5}$
	HDPC		$(4.60 \pm 0.35)\ 10^{-3}$	1.01 ± 0.11	$(1.87 \pm 0.13)\ 10^{-4}$
	Triton X 100		$(3.86 \pm 0.33)\ 10^{-3}$	1.52 ± 0.16	$(6.73 \pm 0.63)\ 10^{-4}$
Indigo Carmine	SDS	$(1.232 \pm 0.014)\cdot10^{-3}$	$(5.89 \pm 0.45)\ 10^{-3}$	2.85 ± 0.26	$(2.08 \pm 0.18)\ 10^{-8}$
	HDPC		$(1.75 \pm 0.19)\ 10^{-2}$	1.75 ± 0.15	$(2.35 \pm 0.21)\ 10^{-4}$
	Triton X 100		$(3.43 \pm 0.24)\ 10^{-3}$	2.96 ± 0.19	$(8.79 \pm 0.72)\ 10^{-3}$

only 15%. In the case of IC/surfactant mixtures, the mineralization degrees were up to 52%, the highest value being achieved in the presence of SDS.

We are well aware of the limitations of BAP oxidation, because increasing the dye/HCO_3^-/H_2O_2 molar ratio above 1/50/50 for CV or 1/25/250 for IC to achieve complete mineralization, may not suit environmentally realistic conditions; therefore, we assume that BAP/surfactant tandem is rather amenable to a pre-treatment step of dye-containing wastewater in a continuous stirred tank reactor (CSTR). In our batch system the decolourization of both dyes was above 60% after 5 min and the, so by keeping the optimized molar ratios dye/surfactant /oxidant and using appropriate stirring and flow conditions in CSTR, high decolourization degrees can be achieved as well. The effluent mixtures would contain drastically decreased TOCs that can reduce significantly the cost impact of subsequent mineralization procedures.

Acknowledgements

This work was supported by a grant of the Romanian National Authority for Scientific Research, CNDI UEFISCDI project number PN-II-PT-PCCA-2011-3.1-0031.

References

[1] E. Forgacs, T. Cserháti, G. Oros, Removal of synthetic dyes from wastewaters: a review, Environ. Int. 30 (2004) 953–971.
[2] P.V. Nidheesh, R. Gandhimathi, S.T. Ramesh, Degradation of dyes from aqueous solution by Fenton processes: a review, Environ. Sci. Pollut. Res. Int. 20 (2013) 2099–2132.
[3] C.-C. Chen, W.-C. Chen, M.-R. Chiou, S.-W. Chen, Y.Y. Chen, H.-J. Fan, Degradation of crystal violet by an FeGAC/H2O2 process, J. Hazard. Mater. 196 (2011) 420–425.
[4] J. Terres, R. Battisti, J. Andreaus, P.C. de Jesus, Decolorization and degradation of Indigo Carmine dye from aqueous solution catalyzed by horseradish peroxidase, Biocatal. Biotransfor. 32 (2014) 64–73.
[5] H. Santoke, W. Song, W.J. Cooper, J. Greaves, G.E. Miller, Free-radical-induced oxidative and reductive degradation of fluoroquinolone pharmaceuticals: kinetic studies and degradation mechanism, J. Phys. Chem. A 113 (2009) 7846–7851.
[6] W. Hua, E.R. Bennett, R.J. Letcher, Ozone treatment and the depletion of detectable pharmaceuticals and atrazine herbicide in drinking water sourced from the upper Detroit River, Ontario, Canada, Water Res. 40 (2006) 2259–2266.
[7] C.E. Noradoun, I.F. Cheng, EDTA Degradation Induced by Oxygen Activation in a Zerovalent Iron/Air/Water System, Environ. Sci. Technol. 39 (2005) 7158–7163.
[8] V. Arantes, A.M.F. Milagres, The effect of a catecholate chelator as a redox agent in Fenton-based reactions on degradation of lignin-model substrates and on COD removal from effluent of an ECF kraft pulp mill, J. Hazard. Mater. 141 (2007) 273–279.
[9] D.E. Richardson, H. Yao, K.M. Frank, D.A. Bennett, Equilibria, kinetics, and mechanism in the bicarbonate activation of hydrogen peroxide: oxidation of sulfides by peroxymonocarbonate, J. Am. Chem. Soc. 122 (2000) 1729–1739.
[10] M. Puiu, T. Galaon, L. Bondilă, A. Răducan, D. Oancea, Feed-back action of nitrite in the oxidation of nitrophenols by bicarbonate-activated peroxide system, Appl. Catal. A-Gen. 516 (2016) 90–99.
[11] A. Xu, X. Li, H. Xiong, G. Yin, Efficient degradation of organic pollutants in aqueous solution with bicarbonate-activated hydrogen peroxide, Chemosphere 82 (2011) 1190–1195.
[12] H. Yao, D.E. Richardson, Epoxidation of alkenes with bicarbonate-activated hydrogen peroxide, J. Am. Chem. Soc. 122 (2000) 3220–3221.
[13] H. Yao, D.E. Richardson, Bicarbonate surfoxidants: micellar oxidations of aryl sulfides with bicarbonate-activated hydrogen peroxide, J. Am. Chem. Soc. 125 (2003) 6211–6221.
[14] D.B. Medinas, G. Cerchiaro, D.F. Trindade, O. Augusto, The carbonate radical and related oxidants derived from bicarbonate buffer, IUBMB Life 59 (2007) 255–262.
[15] M. Bielska, A. Sobczyńska, K. Prochaska, Dye–surfactant interaction in aqueous solutions, Dyes Pigm. 80 (2009) 201–205.
[16] K.V. Roshchyna, S.V. Eltsov, A.N. Laguta, N.O. McHedlov-Petrossyan, Micellar rate effects in the alkaline fading of crystal violet in the presence of various surfactants, J. Mol. Liq. 201 (2015) 77–82.
[17] H.H. Paradies, Shape and size of a nonionic surfactant micelle. Triton X-100 in aqueous solution, J. Phys. Chem. 84 (1980) 599–607.
[18] G. Duplâtre, M.F. Ferreira Marques, M. da Graça Miguel, Size of sodium dodecyl sulfate micelles in aqueous solutions as studied by positron annihilation lifetime spectroscopy, J. Phys. Chem. 100 (1996) 16608–16612.
[19] G. Astray, A. Cid, J.A. Manso, J.C. Mejuto, O.A. Moldes, J. Morales, Alkaline fading of triarylmethyl carbocations in self-assembly microheterogeneous media, Prog. React. Kinet. Mec. 36 (2011) 139–165.
[20] R. Saha, A. Ghosh, B. Saha, Kinetics of micellar catalysis on oxidation of p-anisaldehyde to p-anisic acid in aqueous medium at room temperature, Chem. Eng. Sci. 99 (2013) 23–27.
[21] S. Dasmandal, H.K. Mandal, A. Kundu, A. Mahapatra, Kinetic investigations on alkaline fading of malachite green in the presence of micelles and reverse micelles, J. Mol. Liq. 193 (2014) 123–131.
[22] Y. Zhang, X. Li, J. Liu, X. Zeng, Micellar catalysis of composite reactions—the effect of SDS micelles and premicelles on the alkaline fading of crystal violet and malachite green, J. Disper. Sci. Technol. 23 (2002) 473–481.
[23] A.H. Gemeay, I.A. Mansour, R.G. El-Sharkawy, A.B. Zaki, Kinetics and mechanism of the heterogeneous catalyzed oxidative degradation of indigo carmine, J. Mol. Catal. A-Chem. 193 (2003) 109–120.
[24] C.A. Bunton, The dependence of micellar rate effects upon reaction mechanism, Adv. Colloid Interface Sci. 123–126 (2006) 333–343.
[25] E. Fuguet, C. Ràfols, M. Rosés, E. Bosch, Critical micelle concentration of surfactants in aqueous buffered and unbuffered systems, Anal. Chim. Acta 548 (2005) 95–100.
[26] A. Chatterjee, S.P. Moulik, S.K. Sanyal, B.K. Mishra, P.M. Puri, Thermodynamics of micelle formation of ionic surfactants: a critical assessment for sodium dodecyl sulfate, cetyl pyridinium chloride and dioctyl sulfosuccinate (Na salt) by microcalorimetric, conductometric, and tensiometric measurements, J. Phys. Chem. B 105 (2001) 12823–12831.
[27] S.K. Hait, S.P. Moulik, Determination of critical micelle concentration (CMC) of nonionic surfactants by donor-acceptor interaction with Iodine and correlation of CMC with hydrophile-lipophile balance and other parameters of the surfactants, J. Surfactants Deterg. 4 (2001) 303–309.
[28] H.-J. Fan, S.-T. Huang, W.-H. Chung, J.-L. Jan, W.-Y. Lin, C.-C. Chen, Degradation pathways of crystal violet by Fenton and Fenton-like systems: condition optimization and intermediate separation and identification, J. Hazard. Mater. 171 (2009) 1032–1044.
[29] M.G. Coelho, G.M. de Lima, R. Augusti, D.A. Maria, J.D. Ardisson, New materials for photocatalytic degradation of Indigo Carmine—Synthesis, characterization and catalytic experiments of nanometric tin dioxide-based composites, Appl. Catal B - Environ. 96 (2010) 67–71.
[30] M.L. Chacon-Patino, C. Blanco-Tirado, J.P. Hinestroza, M.Y. Combariza, Biocomposite of nanostructured MnO_2 and fique fibers for efficient dye degradation, Green Chem. 15 (2013) 2920–2928.
[31] I. Dalmázio, A.P.F.M. de Urzedo, T.M.A. Alves, R.R. Catharino, M.N. Eberlin, C.C. Nascentes, R. Augusti, Electrospray ionization mass spectrometry monitoring of indigo carmine degradation by advanced oxidative processes, J. Mass Spectrom. 42 (2007) 1273–1278.
[32] Y. Maruyama, M. Ishikawa, H. Satozono, Femtosecond isomerization of crystal violet in alcohols, J. Am. Chem. Soc. 118 (1996) 6257–6263.
[33] L. García Río, A. Godoy, Influence of CTACl cationic micelles on the spectral behavior of crystal violet, Chem. Phys. 327 (2006) 361–367.
[34] V.B. Gawandi, S.N. Guha, K.I. Priyadarsini, H. Mohan, Steady-state and time-resolved studies on spectral and redox properties of dye-surfactant interactions, J. Colloid Interface Sci. 242 (2001) 220–229.
[35] L. García-Río, P. Hervella, J.C. Mejuto, M. Parajó, Spectroscopic and kinetic investigation of the interaction between crystal violet and sodium dodecylsulfate, Chem. Phys. 335 (2007) 164–176.
[36] C.A. Bunton, M.J. Minch, Micellar effects on the ionization of carboxylic acids and interactions between quaternary ammonium ions and aromatic compounds, J. Phys. Chem. 78 (1974) 1490–1498.
[37] S. Ghosh, S. Mondal, S. Das, R. Biswas, Spectroscopic investigation of interaction between crystal violet and various surfactants (cationic, anionic, nonionic and gemini) in aqueous solution, Fluid Phase Equilib. 332 (2012) 1–6.
[38] S.A. Moore, K.M. Glenn, R.M. Palepu, Spectroscopic investigations on the interaction of crystal violet with nonionic micelles of Brij and Igepal surfactants in aqueous media, J. Solution Chem. 36 (2007) 563–571.

[39] H.-Y. Wang, Hong-Wen Gao, Jian-Fu Zhao, Interaction of Indigo carmine with cetyltrimethylammonium bromide and application to determination of cationic surfactant in wastewater, Bull. Korean Chem. Soc. 24 (2003) 1444–1448.
[40] C.A. Bunton, F. Nome, F.H. Quina, L.S. Romsted, Ion binding and reactivity at charged aqueous interfaces, Acc. Chem. Res. 24 (1991) 357–364.
[41] L.-G. Qiu, A.-J. Xie, Y.-H. Shen, Micellar effects of a triazole-based cationic gemini surfactant on the rate of a nucleophilic aromatic substitution reaction, Colloid Polym. Sci. 283 (2005) 1343–1348.
[42] M.H. Gehlen, M. Ferreira, M.G. Neumann, Interaction of methyl orange with cationic micelles and its effect on dye photochemistry, J. Photoch. Photob. A 87 (1995) 55–60.
[43] R.A. Sheikh, F.M. Al-Nowaiser, M.A. Malik, A.O. Al-Youbi, Z. Khan, Effect of cationic micelles of cetyltrimethylammonium bromide on the MnO4− oxidation of valine, Colloids Surf. A Physicochem. Eng. Asp. 366 (2010) 129–134.
[44] M.A. Malik, S.N. Basahel, A.Y. Obaid, Z. Khan, Oxidation of tyrosine by permanganate in presence of cetyltrimethylammonium bromide, Colloids Surf. B Biointerfaces 76 (2010) 346–353.
[45] A.K. Singh, N. Sen, S.K. Chatterjee, M.A.B.H. Susan, Kinetic study of oxidation of paracetamol by water-soluble colloidal MnO_2 in the presence of an anionic surfactant, Colloid Polym. Sci. 294 (2016) 1611–1622.
[46] K.A. Zachariasse, P. Nguyen Van, B. Kozankiewicz, Investigation of micelles, microemulsions, and phospholipid bilayers with the pyridinium-N-phenolbetaine ET(30), a polarity probe for aqueous interfaces, J. Phys. Chem. A 85 (1981) 2676–2683.
[47] A.M.S. Paulo, C.M. Plugge, P.A. García-Encina, A.J.M. Stams, Anaerobic degradation of sodium dodecyl sulfate (SDS) by denitrifying bacteria, Int. Biodeter. Biodegr. 84 (2013) 14–20.
[48] V. Chaturvedi, A. Kumar, Presence of SDS-degrading enzyme, alkyl sulfatase (SdsA1) is specific to different strains of Pseudomonas aeruginosa, Process Biochem. 48 (2013) 688–693.
[49] H.-J. Chen, D.-H. Tseng, S.-L. Huang, Biodegradation of octylphenol polyethoxylate surfactant Triton X-100 by selected microorganisms, Biores. Technol. 96 (2005) 1483–1491.